

Polystyrene-*b*-poly (acrylic acid) nanovesicles coated by modified chitosans for encapsulation of minoxidil

Gilmar Hanck-Silva^{1*}, Edson Minatti¹

¹Chemistry Department, Federal University of Santa Catarina, Campus Reitor
João David Ferreira Lima, Florianópolis, Santa Catarina, Brazil

In this work, polystyrene-*b*-poly (acrylic acid) (PS-*b*-PAA) nanovesicles were coated by modified chitosans aiming at studying its physicochemical parameters. The chitosan (CS) was chemically modified to add hydrophilic and/or hydrophobic groups, obtaining three modified chitosans. The PS-*b*-PAA nanovesicles were obtained by organic (1,4-dioxane) cosolvent method in water, resulting in nanovesicles with less than 150 nm of diameter (polydispersibility index - PDI at 90° = 0.106), measured by dynamic light scattering (DLS) and transmission electron microscopy (TEM), and negative zeta potential (-37.5 ± 3.2 mV), allowing the coating of its surface with oppositely charged polysaccharides, such as the CS and the modified chitosans. The coating process was made by mixing the colloidal suspensions with the CS and the modified chitosans at specific [CS-x]/[PS-*b*-PAA] ratios (0.001 to 1.0 wt %) and measuring the change in size and surface charge by DLS and zeta potential. Upon reaching maximum adsorption, the zeta potential parameter was positively stabilized ($+26.7 \pm 4.1$ mV) with a hydrodynamic diameter slightly longer (< 200 nm of diameter). The encapsulation efficiency (EE) of minoxidil, quantified by capillary electrophoresis, was 50.7%, confirming their potential as drug delivery carriers and the coating process showed the possibility of controlling the surface charge nature of these nanovesicles.

Keywords: PS-*b*-PAA nanovesicles. Modified chitosan. Coating. Drug delivery system. Minoxidil.

INTRODUCTION

The application of polymers in the development of drug carriers and delivery systems has been extensively studied in the last decades and is motivated mainly by numerous advantages when compared to conventional delivery systems (Sahoo, Parveen, Panda, 2007; Zhang, Chan, Leong, 2013). Some examples include improved bioavailability (Kawashima, 2001), increased therapeutic efficacy (Elgadir *et al.*, 2015), decreased toxicity (Gong *et al.*, 2012; Ojer *et al.*, 2015), improved stability against degradation (Yoon *et al.*, 2013), increased absorption by target sites (Yoon *et al.*, 2013; Kreuter, 2012; Zhang *et al.*, 2016), improved solubility (Kreuter, 2012), controlled release, and specific targeting (Sahoo, Parveen, Panda,

2007; Zhang, Chan, Leong, 2013; Kreuter, 2012; Zhang *et al.*, 2016).

In this sense, copolymers represent a class of macromolecules that are perfectly suitable to prepare nanocarriers due to their ability to self-assemble into well-organized structures. This behavior is due to the incompatibility between the blocks, which, when exposed to mixed selective solvents, generate well-defined macromolecular structures often with distinct hydrophilic and hydrophobic domains (Discher, Eisenberg, 2002; Bellettini *et al.*, 2015), thus allowing the incorporation of drugs of different solubilities (Zhang, Eisenberg, 1995). Despite this, the majority of the studies carried out so far aims at the incorporation of hydrophobic drugs, and the use of hydrophilic drugs is little explored (Bastakoti *et al.*, 2013; Caon *et al.*, 2014).

The diblock copolymer PS-*b*-PAA (Figure 1) self-assembles forming nanostructures with vesicle-like morphology and exhibit negative charges due to the

*Correspondence: G. Hanck-Silva. Departamento de Química. Universidade Federal de Santa Catarina. Campus Reitor João David Ferreira Lima, Bairro Trindade. 88040900 – Florianópolis, Santa Catarina, Brasil. Phone: +55 (48) 37216844. Fax: +55 (48) 37216852. E-mail: gilmar.hanck@gmail.com. ORCID: 0000-0001-8114-6981

protonation of the poly (acrylic acid) (PAA) block in aqueous solution (Discher, Eisenberg, 2002; Bellettini *et al.*, 2015; Dong, Lindau, Ober, 2009). The use of copolymers containing ionizable groups enables the coating of these nanostructures by electrostatic adsorption of opposite-charged polyelectrolytes (Burke, Eisenberg, 2001; Choucair, Lavigueur, Eisenberg, 2004) aiming at improving biocompatibility (Bellettini *et al.*, 2015), permeability (Caon *et al.*, 2014) or even the selective targeting through recognition by specific receptors, for example.

The CS (Figure 2) is a widely studied polyelectrolyte for its biocompatibility and biodegradability properties that in the coating of nanostructures is mainly used to promote skin permeation (Caon *et al.*, 2014; Elgadir *et al.*, 2015). From the chemical point of view, this polyelectrolyte has a large number of amino (ionizable) groups that can be modified to obtain hydrophilic, hydrophobic and/or both (amphiphilic) features. The number of ionizable groups available after chemical modifications enables the change of the level of interaction with the nanostructures, improving the stability and the permeation in the skin.

Minoxidil (Figure 3) is a drug derivative from pyrimidine (6-(1-Piperidiny)-2,4-pyrimidinediamine 3-oxide), hydrophilic, initially used as antihypertensive and approved in the 1980s for the treatment of androgenic alopecia in topical formulations. However, the problem with commercial products is that they contain ethyl alcohol and/or propylene glycol as solvents, which cause severe adverse effects such as irritation and contact dermatitis (Padois *et al.*, 2011). Since then, many studies were performed to develop topical delivery systems for this drug. Many of these systems use organic solvents, so one concern is the elimination of such solvents, which was tested in this study (Shim *et al.*, 2004; Mura *et al.*, 2009; Zhao, Brown, Jones, 2010; Matos *et al.*, 2015). Therefore, the present study aimed at evaluating the influence of chemical modifications in the interaction of different modified chitosans during the coating of PS-*b*-PAA nanovesicles, the application of these nanostructures to the encapsulation of minoxidil, and the elimination of the organic solvent from the systems via two techniques — rotary evaporation and dialysis.

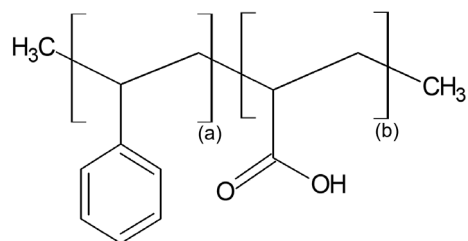


FIGURE 1 - Structural representation of polystyrene-*b*-poly(acrylic acid) (PS-*b*-PAA) diblock copolymer monomer units, where (a) represents the styrene unit and (b) the acrylic acid unit.

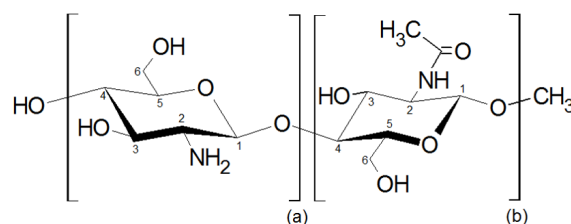


FIGURE 2 - Structural representation of the chitosan monomer units, where (a) represents the deacetylated unit and (b) the acetylated unit with the respective carbon numbers.

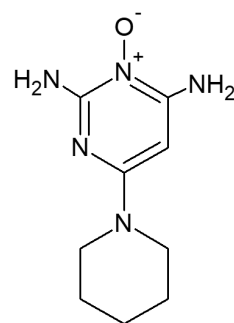


FIGURE 3 - Structural representation of minoxidil.

MATERIAL AND METHODS

Material

The diblock copolymer PS-*b*-PAA was obtained from Polymer Source Inc. (Dorval, Canada) with average degrees of polymerization of 404 and 63 for the PS and the PAA blocks, respectively, with an Mn of PS (45.000 g mol⁻¹) and of PAA (4.500 g mol⁻¹) and polydispersity (weight-average molar mass divided by the number-average molar mass — Mw/Mn) = 1.18. The polysaccharide CS (a linear random copolymer of D-glucosamine and N-acetyl-D-glucosamine) with an Mn of 70.000 g mol⁻¹ (determined by viscosimetry) and

a deacetylation degree (DD) of around 83% (determined by Fourier-transform infrared spectroscopy — FTIR) was purchased from Sigma-Aldrich (St. Louis, United States). The minoxidil (6-(1-Piperidiny)-2,4-pyrimidinediamine 3-oxide) and all other chemicals and reagents were purchased from Sigma-Aldrich (St. Louis, United States) and used without further purification (analytical grade).

Methods

Modified Chitosan with hydrophilic groups

The CS was chemically modified by the insertion of hydrophilic groups (Liu *et al.*, 2006). In brief, 2 g of

the CS was suspended in 30 mL of 2-propanol at room temperature (25 °C) whilst being stirred for 60 min. The resulting suspension was gently mixed with 5.0 mL of NaOH solution (dropwise) at a concentration of 15 M and stirred for 60 min at 25 °C. The mixture containing NaOH was mixed with 10 g of chloroacetic acid at 25 °C while being stirred for 60 min, heated to 60 °C and kept under constant stirring at this temperature for 24 hours. The resulting product was filtered, washed with methanol solution, and dried under reduced pressure to obtain a modified chitosan with a high degree of carboxymethyl substitution. Finally, the resulting molecule was named CS-A or N,O-carboxymethylchitosan, according to Figure 4.

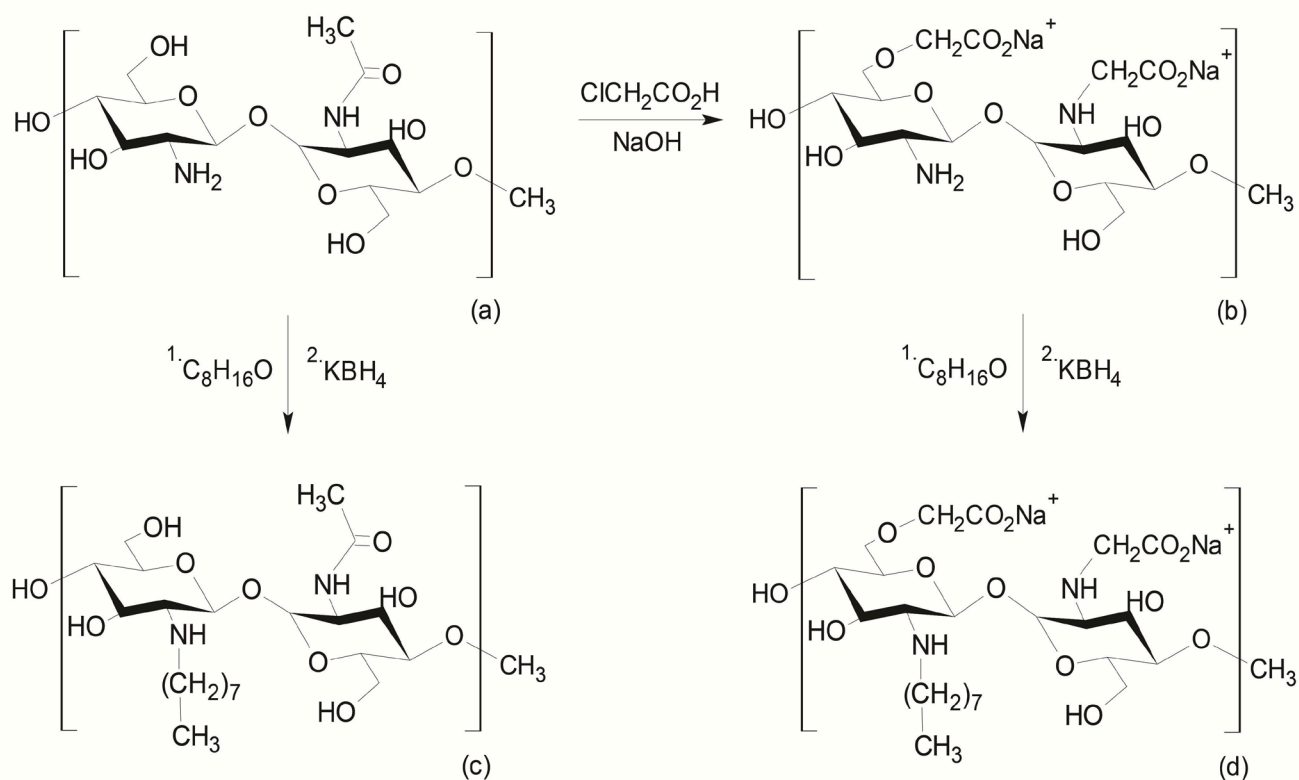


FIGURE 4 - Representation the reactions starting by (a) chitosan (CS) and producing three modified chitosans, (b) N,O-carboxymethylchitosan (CS-A), (c) N-octylchitosan (CS-O) and (d) N,O-carboxymethyl-N-octylchitosan (CS-2).

Modified Chitosan with hydrophobic groups

The CS was chemically modified by the insertion of hydrophobic groups (Qu *et al.*, 2013). So, 1 g of the CS was suspended in 30 mL of methanol. This suspension was stirred vigorously at room temperature (25 °C) for 60 min, then 1 g of octanal was dropped into the suspension and the mixture was stirred at 30 °C for 4 hours. After this time, it was mixed with 5.0 mL of a solution of potassium borohydride (KBH₄) at 0.1 g ml⁻¹ and kept under constant stirring for 4 hours at 30 °C. The resulting product was filtered, washed with water, methanol, and diethyl ether and dried under reduced pressure to obtain a modified chitosan that was named CS-O or N-octylchitosan, according to Figure 4.

Modified Chitosan with amphiphilic groups

The modified chitosan with hydrophilic groups was utilized for the addition reaction to hydrophobic groups, thus obtaining the amphiphilic-chitosan modified with both hydrophilic and hydrophobic groups that were named CS-2 or N,O-carboxymethyl-N-octylchitosan, as shown in Figure 4.

PS-*b*-PAA nanovesicles

The PS-*b*-PAA nanovesicles were prepared using the cosolvent self-assembly method. This copolymer was initially dissolved in 1,4-dioxane (a common solvent for both blocks of the copolymer) at 0.5 wt % and 25 °C. The incorporation of minoxidil was performed using different drug concentrations in ultrapure water (ranging from 0.001 to 0.1 wt %) that was dropwise added to the solution of copolymer in 1,4-dioxane (until a content of 50 wt % was obtained) at a rate of 250 μL h⁻¹, using a syringe pump (SAMTRONIC ST670 - São Paulo, Brazil) under constant magnetic stirring (1000 rpm) to induce the self-assembly. The colloidal suspension was then quenched with a 10-fold excess of highly purified water under constant magnetic stirring. Two methods were tested to remove the organic solvent: the first using a rotary evaporator under reduced pressure and the second dialyzing

against distilled water for 2 days using a membrane with MWCO ≈ 3500 g mol⁻¹ (Spectra/Pro 6).

Coating PS-*b*-PAA nanovesicles with modified chitosans

The CS and the modified chitosans were dissolved overnight in a buffer solution (0.2 acetic acid/0.1 sodium acetate, pH = 4.5), bearing positive charges arising from the free amino groups present in its backbone. For the coverage of the PS-*b*-PAA nanovesicles bearing negative groups (arising from the acrylic acid groups ionized in distilled water pH, pka = 4.26 (Dong, Lindau, Ober, 2009)) specific volumes of PS-*b*-PAA suspensions and modified chitosans solutions were mixed under constant magnetic stirring for 30 min. Different [CS-*x*]/[PS-*b*-PAA] ratios (ranging from 0.001 to 1.0 wt %) were mixed to determine the amount of polycation required for complete coverage of the nanovesicles. The coated nanovesicles were denominated CS/PS-*b*-PAA, CS-A/PS-*b*-PAA, CS-O/PS-*b*-PAA, and CS-2/PS-*b*-PAA respectively, according to the modified chitosans utilized.

Characterization

Chitosan chemical modification: Infrared spectroscopy (FTIR) and Titrations (Conductometric and Potentiometric)

The infrared spectroscopy and the titrations (conductometric and potentiometric) were utilized for determining the DD and the substitution degree (SD) of the CS and of the three modified chitosans. For determining the DD of the CS in FTIR a relationship of

$$(1) \quad DD = 100 \left[1 - \left(\frac{A_{1655}}{A_{3340}} \right) \cdot \left(\frac{1}{1.33} \right) \right]$$

was used, where A is the absorbance at the particular wave number to the two points of absorption (1655 and 3340 cm⁻¹) that correspond to the amide and primary amine groups of the CS, respectively. The factor (1.33) represents the value of the ratio A₁₆₅₅/A₃₃₄₀ to the fully N-acetylated chitosan (El-Sherbiny, 2009). The infrared spectra of the unmodified and of the modified chitosans (KBr pellets) were obtained using a Shimadzu IR Prestige FTIR

spectrophotometer, operating in the range 4000–400 cm^{-1} with a resolution of 2 cm^{-1} . The DD of the CS and, mainly, the SD of the modified chitosans were determined by conductometric and potentiometric titration, combined for comparison, according to the procedures described in the literature (Ge, Luo, 2005; Abreu, Campana-Filho, 2005) and calculated according to the equations:

$$(2) \quad \text{DD} = \left(\frac{161 \cdot [\text{NaOH}] \cdot [v_2 - v_1]}{m} \right) \cdot 100$$

$$(3) \quad \text{SD} = \left(\frac{161 \cdot [\text{NaOH}] \cdot [v_2 - v_1]}{m - (\text{Mw} \cdot [\text{NaOH}] \cdot [v_2 - v_1])} \right) \cdot 100$$

where 161 is the molar mass of glucosamine (the CS skeleton unit), $[\text{NaOH}]$ is the concentration of NaOH (mol L^{-1}), v is the volume of NaOH required to reach the inflection point (L), m is the mass of sample (g) and Mw is the molar masses of derivatizing groups (42 = acetyl group; 58 = carboxymethyl group; 112 = octyl group).

Dynamic light scattering (DLS)

The hydrodynamic diameter (D_H) values of the bare PS-*b*-PAA nanovesicles, as well as the different [CS-*x*]/[PS-*b*-PAA] systems, were measured using an ALV/CGS-3 goniometer, which consists of a 22 mW HeNe linear polarized laser operating at a wavelength of 632.8 nm with a digital correlator of 125 ns initial sampling time, and a temperature controller. DLS data were collected for 1.0 mL of PS-*b*-PAA nanovesicle suspension (0.025 mg mL^{-1}) or the solution mixtures containing specific [CS-*x*]/[PS-*b*-PAA] ratios (ranging from 0.001 to 1.0) at 25 °C recorded over 300 s for each angle (ranging from 30° to 150°). For suspensions of spherical particles, the Stokes-Einstein equation is adequate to describe the relationship between the hydrodynamic particle size (D_H) and the diffusion coefficient (D) and it is given as:

$$(4) \quad R_H = \frac{K_B T}{(6\pi\eta D)}$$

where R_H is the hydrodynamic radius, K_B is the Boltzmann constant, T is the sample temperature and η is the viscosity.

Zeta potential (ζ)

The zeta potential (ζ) values of the bare PS-*b*-PAA nanovesicles, as well as the different [CS-*x*]/[PS-*b*-PAA] ratio systems, were measured using a NanoZS Zetasizer (Malvern Equipments). Similarly, to the procedure reported in previous section, 1.0 mL of the PS-*b*-PAA nanovesicle suspension (0.025 mg mL^{-1}) or the solution mixture containing specific [CS-*x*]/[PS-*b*-PAA] ratios (ranging from 0.001 to 1.0) was measured using a folded capillary zeta cuvette (DTS1070) in triplicate at 25 °C.

Transmission electron microscopy (TEM)

The morphology and particle size distribution of the PS-*b*-PAA nanovesicles and the solution mixture of the [CS-*x*]/[PS-*b*-PAA] were investigated using transmission electron microscopy (TEM). All samples were observed using a TEM 100 kV JEM-1011 microscope operating at an acceleration voltage of 80 kV. The aqueous suspensions (5.0 μL) were dropped onto the Cu grids (200 mesh) covered with a thin layer of carbon. Water was allowed to evaporate from the grids at atmospheric pressure and room temperature. Images were captured at different magnifications.

Capillary Electrophoresis (CE) analysis

The EE (%) was estimated by measuring the difference between the total amount of minoxidil added to the nanoparticle suspensions and the amount of non-loaded minoxidil remaining in the supernatant of the solution after an ultrafiltration procedure at 14000 rpm for 60 min. Aliquots (20 μL) of these solutions were injected into the Capillary Electrophoresis system and the drug content was expressed in $\mu\text{g mL}^{-1}$ suspension. The EE was expressed in percent concentration, which is given as:

$$(5) \quad \text{EE}(\%) = \frac{(C1 - C2)}{C1} \cdot 100$$

where C1 is the initial concentration and C2 is the free concentration in solution supernatant.

The EE was analyzed using a capillary electrophoresis instrument (model CE^{3D}; Agilent Technologies) equipped with a UV diode array detector and HP ChemStation software version Rev. B.04.02(96) for control, processing, and acquisition of data. Electrophoretic measurements were performed on an uncoated fused silica capillary (Polymicro Technologies) with a total length of 48.5 cm (50 μm i.d. and 375 μm o.d.). The capillary was pre-conditioned with a solution of 1.0 M NaOH, deionized water, and background electrolyte (BGE) for 5 min, consecutively. The BGE was composed of 20 mM of glycine and 20 mM of malic acid (pH 3.0). The capillary was flushed for 1 min with BGE between runs. A working solution of a minoxidil standard and a stock solution of imidazole were prepared in deionized water (50 mg L⁻¹). Calibration curves were obtained after preparing individual standards in concentrations from 0.5 to 90 ppm. Standard solutions and samples were introduced from the capillary inlet end (length to the detector: 40 cm) and injected hydrodynamically at 50 mbar for 5 s (50 mbar = 4996.2 Pa). The separation was performed applying a positive voltage of +30 kV. The detection wavelength was maintained at 288 nm and the capillary chamber was set at 25 °C for all the experiments.

Residual solvent assessed using GC-MS analysis

The elimination of the organic solvent was tested using a Shimadzu GCMS-2010 gas chromatograph equipped with a split/splitless injector and an Agilent Technologies DB-5MS column (30 m x 0.25 mm x 0.25 μm film thickness). The oven temperature program was as follows: 50 °C (3 min), 10 °C/min to 250 °C (5 min). The helium carrier gas flow rate was 1.5 mL min⁻¹ in split mode. The temperature of the transfer line and that of the electron impact ion source (70 eV) were fixed at 250 °C. MS was performed in full-spectrum scanning mode (15 to 400 m/z). The dialyzing and evaporated samples were placed in vials and extracted by solid-phase microextraction (SPME) with 7- μm CAR-PDMS fibers (Supelco). The fibers were exposed to the headspace of the samples and kept at room temperature for 30 min, retracted into a needle, and introduced into the gas chromatograph.

RESULTS AND DISCUSSION

Modified Chitosans: synthesis and characterization

The modified chitosans were characterized by FTIR and the SD, for each group entered, as estimated by potentiometric and conductimetric titration, simultaneously. Figure 5 shows the FTIR spectra of the CS and its derivatives.

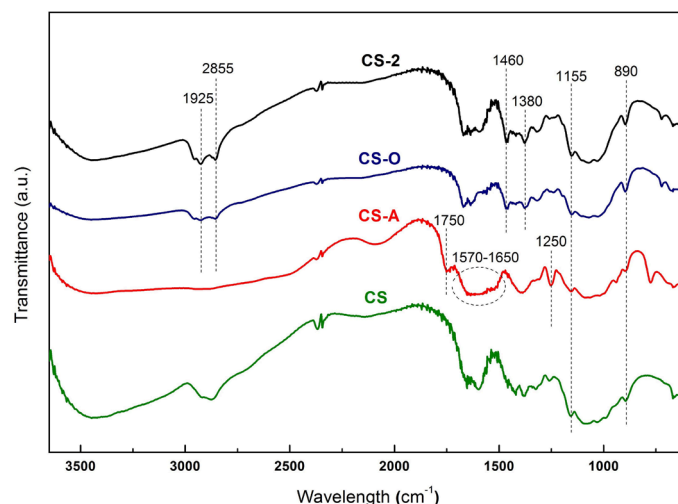


FIGURE 5 - FTIR spectra of CS, CS-A, CS-O, and CS-2.

As can be seen, all spectra showed the characteristic bands of a polysaccharide structure in the region 890–1155 cm^{-1} . For the CS-A derivative, there was an increase at the intensity of the characteristic band of the alcohol function (C-O) at 1250 cm^{-1} and an enlargement of the secondary amine referring band between 1570–1650 cm^{-1} . For the CS-O and the CS-2 derivatives, there was an increase at the intensity of the angular stretch C-H at 1380 cm^{-1} and there was an increase at the intensity of the bands of the aliphatic C-H asymmetric stretch at 2855 cm^{-1} and at 2925 cm^{-1} . In addition, there was a shift of the band of the axial amide stretch (C-N) from 1420 cm^{-1} in the CS to 1460 cm^{-1} , and there was a displacement and intensity decrease of the band of the axial stretch of C=O (1655 cm^{-1} in the CS) for all derivatives, but especially for the CS-A derivative (1750 cm^{-1}). Results agree with those previously reported in the literature (Liu *et al.*, 2006; Mourya, Inamdar, 2008; Huo *et al.*, 2010; Qu *et al.*, 2013), which confirmed the occurrence of the CS modification reactions through the insertion of hydrophilic, hydrophobic, and amphiphilic groups, respectively.

The potentiometric and conductimetry techniques are commonly used to determine the SD of a polymer after the chemical modification reaction. As the CS, the derivatives produced by modification reactions are weak polyelectrolytes containing carboxyl and amine groups distributed along the polymeric structure. So, these techniques can be used to assess the behavior of modified chitosans in a solution depending on the pH and the conductivity of the medium. Thus, the SD of the modified chitosans was calculated using the equation of SD for the second derivative method and obtained, according to the polled groups in the following results, as shown in Table I.

Both titration techniques are quite similar, so the results showed no significant differences. As can be seen, there was a high SD of carboxymethyl groups in the insert, which improved the solubility of the derivative (CS-A) in water compared with the CS alone. In the insertion octyl groups (alkyls with 8 carbons), a minor SD was intended so that there was a great impairment in the solubility of the CS-O derivative. Finally, it can be observed that despite using the same

method and reaction time, the SD for the CS-2 derivative has been halved, as expected, because this reaction utilized the CS-A derivative and not the CS, so the former had fewer sites free for modification, leading to a reduction in the SD.

TABLE I-Substitution degree (SD) obtained by potentiometry and conductimetry for modified chitosans

Chitosan derivative (Researched group)	Potentiometry (%)	Conduitimetry (%)
CS-A (Carboxymethyl)	54.05 ± 0.42	55.16 ± 0.61
CS-O (Octyl)	10.75 ± 0.37	11.38 ± 0.52
CS-2 (Octyl)	5.33 ± 0.59	5.83 ± 0.54

Coating PS-*b*-PAA nanovesicles: change in particle size, surface charge, and morphology

The coating process of the PS-*b*-PAA nanovesicles was carried out by simply mixing these nanovesicles suspensions with the CS-*x* solutions in different concentrations (ranging from 0.001 to 1.0 wt %). This coating of PS-*b*-PAA nanovesicles is ruled by electrostatic interactions between negative groups of PAA and the positive charges from modified polyelectrolytes (CS-*x*). These interactions depend mainly on the particle surface charge, allowing these dynamic changes to be measured by zeta potential and thereby allowing us to infer the occurrence of interactions by the change on the surface charge when these charged particles form complexes with polyelectrolytes. This measurement informs the electrostatic repulsion and the stability of such suspensions (Bellettini *et al.*, 2015). In addition, these changes can also be estimated from DLS measurements and observed by TEM images.

The electrostatic forces of attraction and repulsion from the coating of the PS-*b*-PAA nanovesicles with polyelectrolytes of the CS-*x* resulted, in low CS-*x* concentrations, in size and PDI values close to those obtained for the uncoated nanoparticles, as shown in Tables II-VI.

Table II - Mean diameter, polydispersity index (PDI) and zeta potential for uncoated nanovesicles and minoxidil-loaded and uncoated nanovesicles with analysis of variance (ANOVA) between samples.

Parameters	Uncoated nanovesicles	Minoxidil-loaded and uncoated nanovesicles	ANOVA
Mean diameter (nm)	147 ± 4.2	148 ± 3.9	0.7676
PDI	0.106	0.103	0.3029
Zeta potential (mV)	- 37.5 ± 3.2	- 36.7 ± 4.1	0.9205

Table III - Mean diameter, polydispersity index (PDI) and zeta potential for chitosan-coated nanovesicles without and with minoxidil (CS/PS-*b*-PAA - chitosan/nanovesicles ratio: initial - 0.001; aggregate - between 0.01 and 0.08, with a peak at 0.03; finish - 1.0) with analysis of variance (ANOVA) between samples.

Parameters	(CS/PS- <i>b</i> -PAA) without minoxidil			(CS/PS- <i>b</i> -PAA) with minoxidil			ANOVA		
	Initial	Aggregate	Finish	Initial	Aggregate	Finish	Initial	Aggregate	Finish
Mean diameter (nm)	157 ± 5.4	1636 ± 50	198 ± 4.3	155 ± 4.7	1623 ± 68	201 ± 3.7	0.9512	0.7006	0.2935
PDI	0.102	0.529	0.081	0.108	0.458	0.151	0.9999	0.5802	0.9334
Zeta potential (mV)	- 17.4 ± 1.8	- 0.7 ± 1.7	+ 26.4 ± 3.1	- 18.2 ± 2.3	- 0.5 ± 3.2	+ 25.7 ± 2.9	0.7245	0.8334	0.6836

Table IV - Mean diameter, polydispersity index (PDI) and zeta potential for chitosan derivative-coated nanovesicles without and with minoxidil (CS-A/PS-*b*-PAA - N,O-carboxymethylchitosan/nanovesicles ratio: initial - 0.001; aggregate – between 0.02 and 0.1, with a peak at 0.05; finish - 1.0) with analysis of variance (ANOVA) between samples.

Parameters	(CS-A/PS- <i>b</i> -PAA) without minoxidil			(CS-A/PS- <i>b</i> -PAA) with minoxidil			ANOVA		
	Initial	Aggregate	Finish	Initial	Aggregate	Finish	Initial	Aggregate	Finish
Mean diameter (nm)	158 ± 4.2	1542 ± 44	205 ± 2.5	160 ± 3.5	1554 ± 53	201 ± 1.9	0.7049	0.7517	0.4480
PDI	0.104	0.688	0.094	0.111	0.578	0.099	0.4000	0.3420	0.2175
Zeta potential (mV)	- 18.9 ± 3.1	- 0.1 ± 4.6	+ 23.0 ± 4.1	- 17.6 ± 3.6	- 0.2 ± 4.1	+ 22.4 ± 3.7	0.2079	0.1875	0.6214

Table V - Mean diameter, polydispersity index (PDI) and zeta potential for chitosan derivative-coated nanovesicles without and with minoxidil (CS-O/PS-*b*-PAA - N-octylchitosan/nanovesicles ratio: initial - 0.001; aggregate - between 0.02 and 0.15, with a peak at 0.06; finish - 1.0) with analysis of variance (ANOVA) between samples.

Parameters	(CS-O/PS- <i>b</i> -PAA) without minoxidil			(CS-O/PS- <i>b</i> -PAA) with minoxidil			ANOVA		
	Initial	Aggregate	Finish	Initial	Aggregate	Finish	Initial	Aggregate	Finish
Mean diameter (nm)	151 ± 3.4	1610 ± 88	194 ± 6.4	153 ± 3.8	1604 ± 68	197 ± 3.8	0.5384	0.7491	0.6341
PDI	0.105	0.499	0.131	0.109	0.475	0.113	0.5909	0.4896	0.9221
Zeta potential (mV)	- 17.0 ± 1.1	- 0.6 ± 3.2	+ 27.4 ± 4.7	- 16.7 ± 1.4	- 0.3 ± 2.7	+ 28.8 ± 3.4	0.7045	0.4688	0.2910

Table VI - Mean diameter, polydispersity index (PDI) and zeta potential for chitosan derivative-coated nanovesicles without and with minoxidil (CS-2/PS-*b*-PAA - N,O-carboxymethyl-N-octylchitosan/nanovesicles ratio: initial - 0.001; aggregate – between 0.03 and 0.2, with a peak at 0.15; finish - 1.0) with analysis of variance (ANOVA) between samples.

Parameters	Coated nanovesicles (CS-2/PS- <i>b</i> -PAA)			Coated nanovesicles (CS-2/PS- <i>b</i> -PAA)			ANOVA		
	Initial	Aggregate	Finish	Initial	Aggregate	Finish	Initial	Aggregate	Finish
Mean diameter (nm)	161 ± 3.8	1505 ± 58	197 ± 4.4	159 ± 4.2	1522 ± 74	195 ± 4.2	0.7647	0.7374	0.7741
PDI	0.101	0.483	0.098	0.103	0.536	0.108	0.2500	0.4853	0.1856
Zeta potential (mV)	- 16.3 ± 2.1	- 0.03 ± 5.3	+ 25.5 ± 4.5	- 17.3 ± 3.0	- 0.1 ± 4.8	+ 24.3 ± 3.7	0.2195	0.4842	0.9384

The zeta potential values were initially less negative compared to uncoated systems. However, when the concentrations of the CS-*x* polyelectrolyte increased, the formation of aggregates on the micrometers order

was observed in a concentration range up to a maximum, passing through a transition region near the neutralization point (zero potential), which was observed both by DLS and zeta potential, as shown in Figure 6.

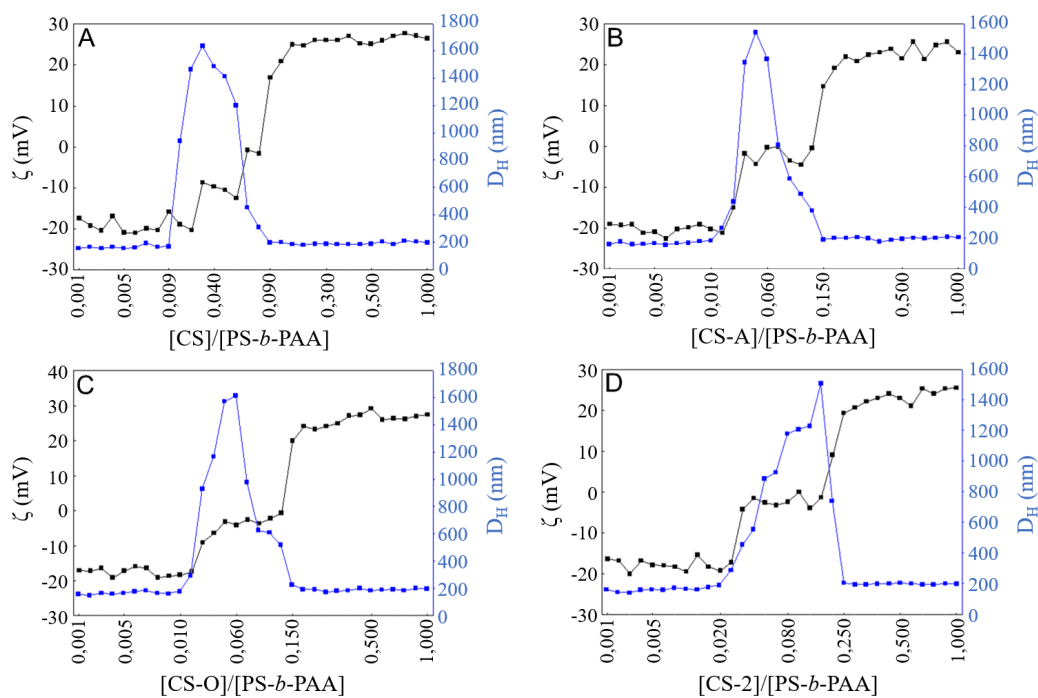


FIGURE 6 - Change of D_H (nm) and ζ (mV) values as a function of $[CS-x]/[PSb-PAA]$ ratio: (A) CS (B) CS-A (C) CS-O and (D) CS-2.

A maximum particle size was observed for all systems (right axis in Figure 6 A-D) indicating aggregation of the coated vesicles, which resulted from the polyelectrolyte complexation between the nanovesicles surface charge and the CS-x. This complexation was the result of the neutralization of both charges, both the negative nanovesicles and the positive charge of the CS-x. As the amount of polyelectrolytes CS-x was increased, the size of the nanovesicles decreased again, remaining slightly larger than uncoated nanovesicles. This clearly indicates a saturation of the CS-x molecules adsorbed on the PS-*b*-PAA nanovesicles surface that now has the same charge as the surrounding ones, resulting in electrostatic repulsion and stabilization of the suspension medium, as confirmed by the zeta potential measurements (left axis in Figure 6 A-D). This shows an inversion from negative potential (uncoated PS-*b*-PAA nanovesicles) to positive potential values as the CS-x complexes with the nanovesicles surface, moving towards a neutral point (zero potential) from the particle aggregation.

As expected, there are differences between the adsorption profiles on the surface of the PS-*b*-PAA nanovesicles for each tested polysaccharide. Since the CS has a greater number of ionizable groups available, it interacts more than the other derivatives produced, requiring a lower concentration of the CS to saturate the entire nanovesicles surface. The exact same amount of the CS-A and the CS-O derivatives were necessary for complete coverage of nanovesicles and consequently, a higher concentration of CS-2 was necessary, precisely because it has a greater number of substituted ionizable groups.

The morphology of the nanoparticles was investigated by transmission electron microscopy (TEM). Figure 7 (A-B) shows the formation of well-defined nanovesicles with dimensions around 150 nm. The PS-*b*-PAA nanovesicles have great contrast in TEM, making it clearly possible to highlight their morphology. This happens because the PS block has an electron density greater than the PAA block, enabling the hydrophobic block to be observed in the darkest region of the micrograph since the hydrophilic block is often not visible (Mai, Eisenberg, 2012).

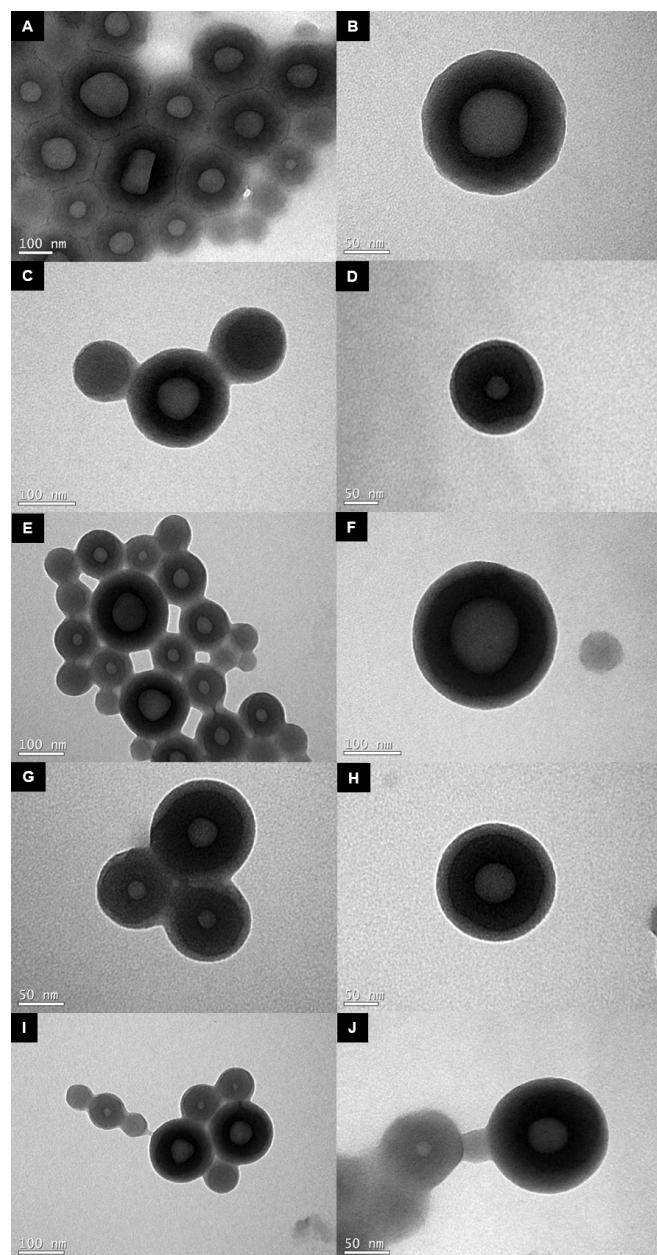


Figure 7 - TEM images of PS-*b*-PAA nanovesicles prepared by the co-solvent method (1,4-dioxane/water). Nanovesicles without coating and without drug (A), nanovesicles without coating and with minoxidil (B), nanovesicles CS coated without drug (C) and with minoxidil (D), nanovesicles CS-A coated without drug (E) and with minoxidil (F), nanovesicles CS-O coated without drug (G) and with minoxidil (H), nanovesicles CS-2 coated without drug (I) and with minoxidil (J). Scale bar of 100 nm (higher magnification) and 50 nm (lower magnification), respectively.

The coating of these nanovesicles can be seen in Figure 7 (C-J), which shows that there are differences on a superficial level on the adsorption of the CS and of the

modified chitosans in the nanovesicles, represented by a clearer outer layer. Unlike measurements of DLS and zeta potential, the TEM images show no clearly visible morphological differences between the adsorption of the CS and other modified chitosans and the encapsulation of minoxidil did not lead to visible morphological changes nor significant changes in size and zeta potential parameters when compared to the systems without the substance, as shown in Tables II - VI.

Encapsulation and residual organic solvent

The initial concentrations of PS-*b*-PAA and minoxidil were 0.5 and 0.012 wt %, respectively. Although different substance concentrations ranging from 0.001 to 0.1 have been tested, this polymer/substance ratio was selected since it provided a higher EE (approximately 50%). The calibration curve showed that the method developed by capillary electrophoresis was linear with a correlation coefficient of 0.999. It showed detection and quantification limit values of 0.08 and 0.24 $\mu\text{g ml}^{-1}$, respectively, indicating that it was sufficiently sensitive to the quantitation of minoxidil.

Minoxidil is a hydrophilic substance (Zhao, Brown, Jones, 2010) and since these polymer systems are developed in water, the minoxidil can be found either inside the nanovesicles (encapsulated), externally (in coating), interacting with the surface charges both on the copolymer and on the CS-x, or stay in the solution, causing a maximum EE of 50.7%, which was considered a great result (Figure 8-10).

Despite considering minoxidil for topical use, it can be used orally for the treatment of resistant hypertension in cases where the therapy with multidrug regimens fails (Sica, 2004). The coating with the chitosan and its derivatives, in turn, can be used for several biomedical applications (Frank *et al.*, 2020) such as increasing skin adhesion and penetration (Jung *et al.*, 2015), as well as oral absorption of drug delivery systems (Sheng *et al.*, 2015).

Many pharmaceuticals and drug delivery systems are developed using organic solvents, so the removal of these residual solvents and its quantification through appropriate analytical methods is of great concern (Zhang, Fang, Liang, 2019). In this sense, the first

legislation to address the issue was created in 1996 by the International Conference on Harmonization (ICH) with the ICH Q3C guideline, called “Impurities: Guideline for residual solvents”, currently in its sixth revision. This guideline presents the classification of residual solvents, according to the available toxicity data, classifying them in 3 categories (International Conference on Harmonization, 2019). Following the ICH, some pharmacopeias have published specific general chapters on monitoring residual solvents in excipients and pharmaceuticals, such as the United States Pharmacopeia (USP) in its general chapter “<467> Residual Solvents” (United States Pharmacopeia, 2007).

According to the ICH Q3C guidelines, 1,4-dioxane is classified as a class 2 residual solvent, that is, non-

genotoxic animal carcinogenic, and its use should be limited in pharmaceutical products due to its inherent toxicity (International Conference on Harmonization, 2019). Thus, two methods were tested and analyzed by GC-MS to verify the elimination of 1,4-dioxane. The dialysis process completely removed 1,4-dioxane, unlike the evaporation process that left some 1,4-dioxane residue, even though less than 0.01% (100 ppm), within the acceptable limit of 380 ppm. This shows that both methods were effective in eliminating the residual Organic solvent (Figure 8-10).

The next steps proposed in this research include the analysis by NMR to confirm more accurately the SD of the inserted groups and performing release studies, toxicity, and skin permeation of these developed systems.

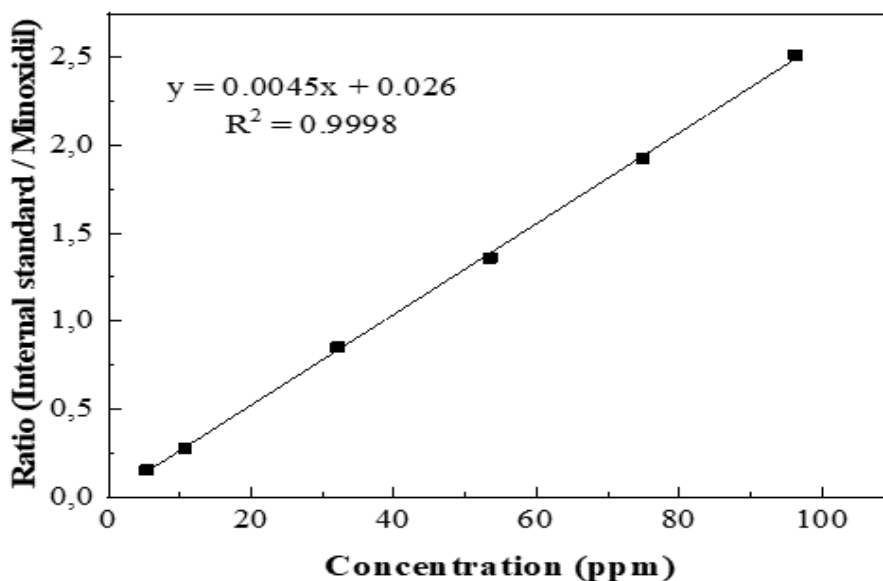


Figure 8 - Linear calibration curves obtained by varying the concentration of minoxidil 0.5-90 ppm. Separation conditions: fused silica capillary, 50 μm i.d., 375 μm o.d., 48.5 cm total length (8.5 cm to detector); electrolyte: 20 mM of glycine and 20 mM of malic acid, pH 3.0; voltage: + 30 kV; hydrodynamic injection: 5 s x 50 mbar; indirect UV absorbance detection at 288 nm; temperature: 25 $^{\circ}\text{C}$.

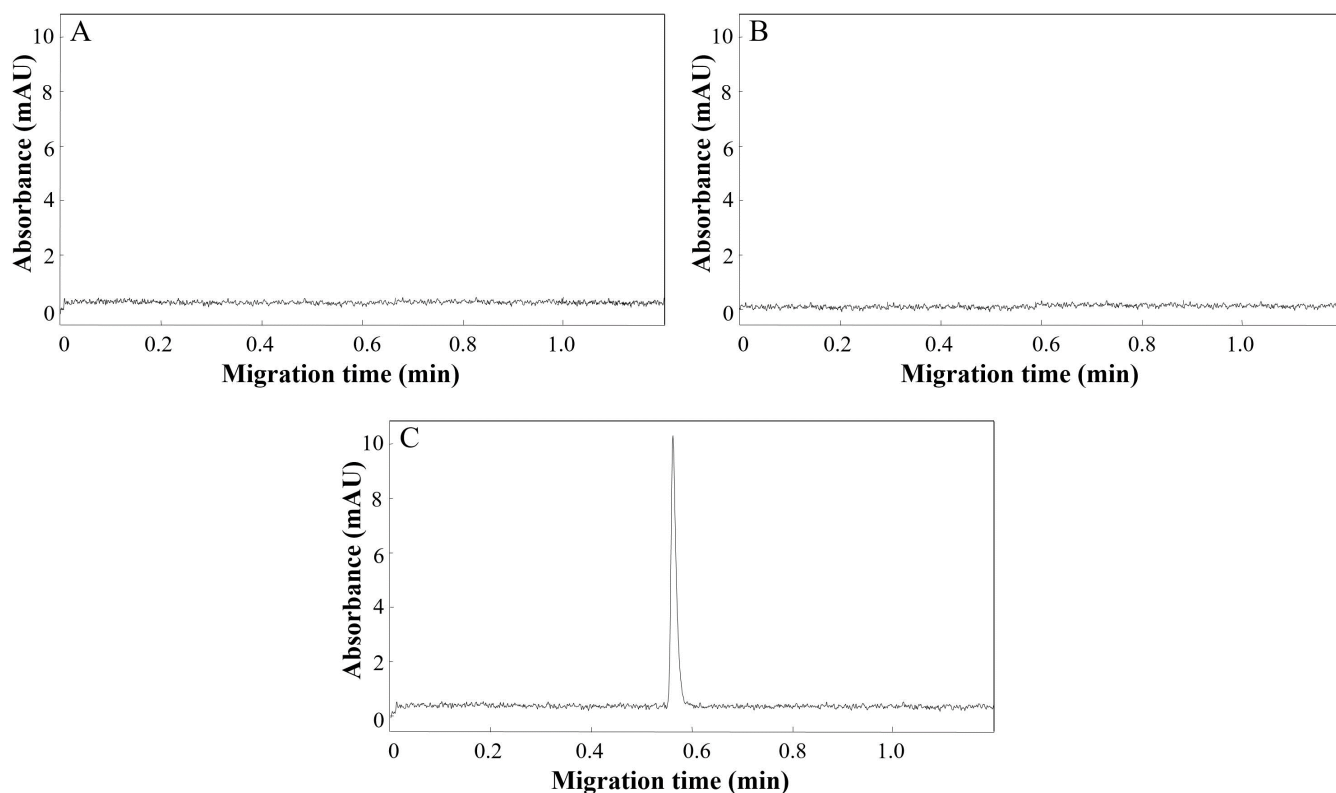


Figure 9 - Electropherograms of the empty nanovesicles (A), only coated with chitosan (B) and encapsulated with minoxidil (C). Separation conditions: fused silica capillary, 50 μm i.d., 375 μm o.d., 48.5 cm total length (8.5 cm to detector); electrolyte: 20 mM of glycine and 20 mM of malic acid, pH 3.0; voltage: + 30kV; hydrodynamic injection: 5 s x 50 mbar; indirect UV absorbance detection at 288 nm; temperature: 25 $^{\circ}\text{C}$.

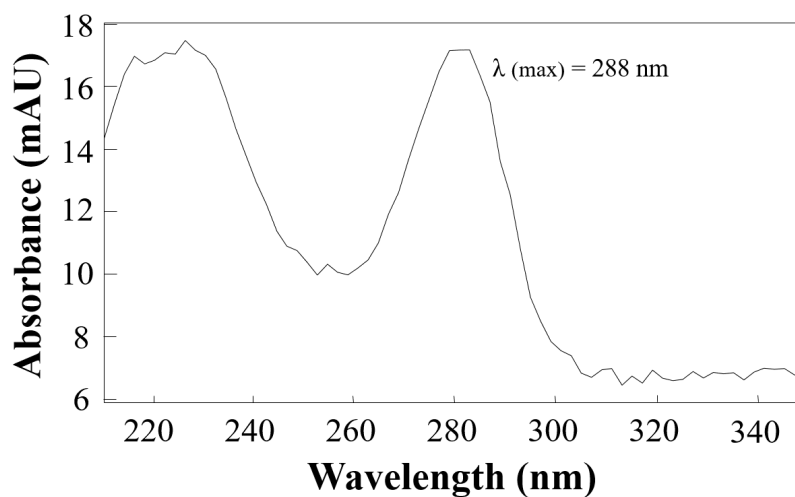


Figure 10 - UV-Vis absorption spectrum of minoxidil.

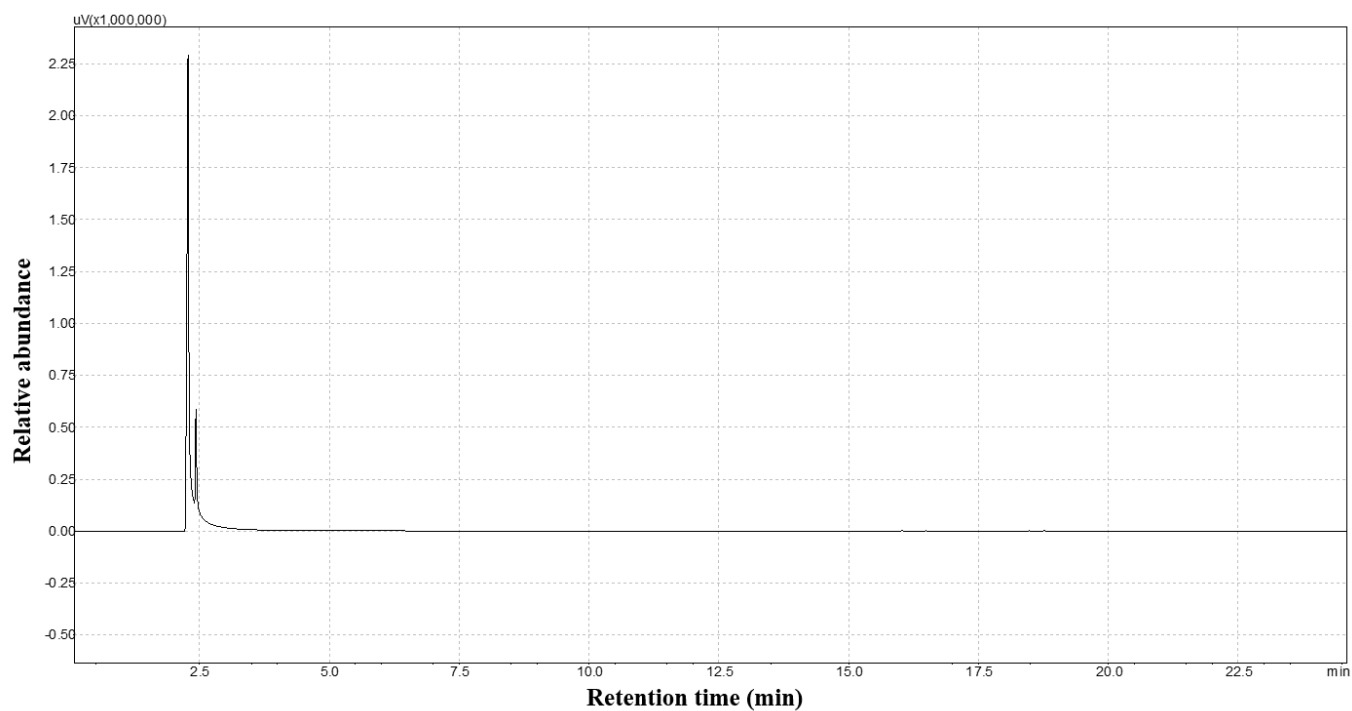


Figure 11 - GC-MS chromatogram of 1,4-dioxane standard.

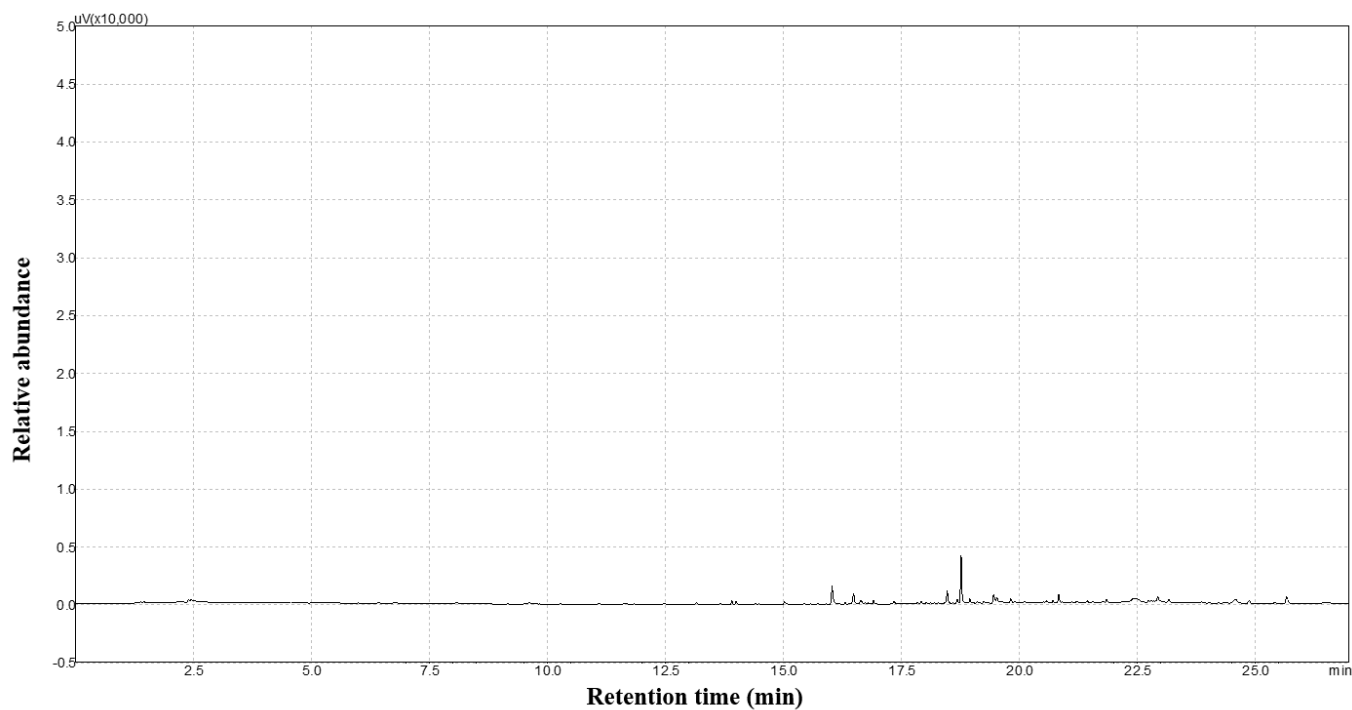


Figure 12 - GC-MS chromatogram of dialyzed nanovesicles.

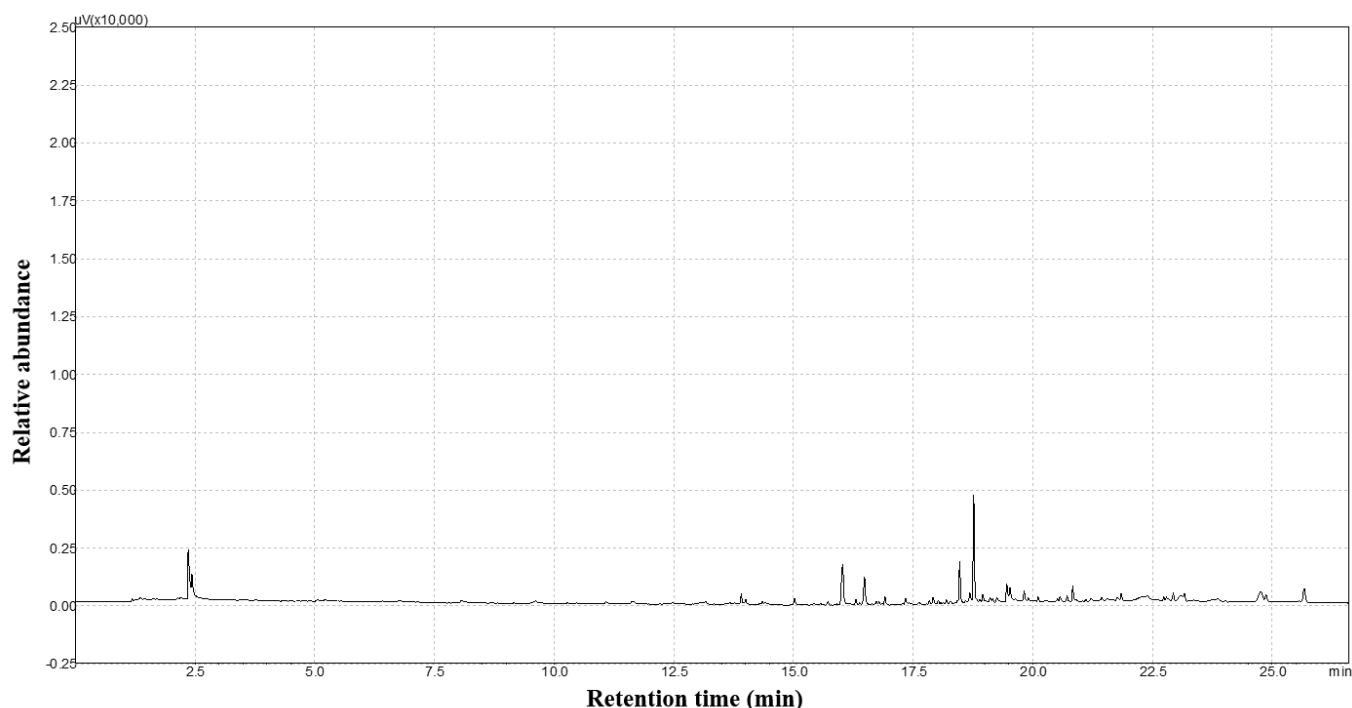


Figure 13 - GC-MS chromatogram of rotary evaporated nanovesicles.

CONCLUSIONS

The chemical modification of the CS to obtain derivatives with distinct characteristics of hydrophilicity was successfully achieved. As evidenced, the co-solvent method is efficient to self-assemble the PS-*b*-PAA copolymer chains into vesicles, producing nanovesicles with diameters smaller than 150 nm, low polydispersity, and negative surface charge arising from PAA ionizable groups, allowing the coating with other polyelectrolytes of positive charge, for example, the CS and its derivatives. DLS and zeta potential data showed significant changes in size and surface charge due to the coating process and there were also changes in morphology as observed by TEM, indicating that the coating of these nanovesicles was successfully achieved through electrostatic interactions using the CS and the modified chitosans. Encapsulation of minoxidil, both in the uncoated as coated nanovesicles, generated a maximum satisfactory EE since minoxidil is soluble in water. The dialysis process managed to completely eliminate the residual organic solvent from the systems; even though the evaporation process leaves

a remainder, it is within the acceptable limit. The coated nanovesicles with the CS and different modified chitosans had hydrodynamic diameter (D_H) slightly larger than the uncoated nanovesicles and the surface became positively charged with the coating processes. Thus, the coating process with the modified chitosans interacts differently according to the chemical group inserted and indicated that it is possible to control the surface charge (negative or positive) and thereby improve the stability of these systems.

ACKNOWLEDGMENTS

The authors would like to acknowledge CAPES and CNPq for financial support and Laboratório Central de Microscopia Eletrônica (LCME) at Universidade Federal de Santa Catarina (USFC) for the microscopy analyzes.

REFERENCES

Abreu FR, Campana-Filho SP. Preparation and characterization of carboxymethylchitosan. *Polímeros*. 2005;15(2):79-83.

- Bastakoti BP, Liao S-H, Inoue M, Yusa S-I, Imura M, Nakashima K, et al. pH-responsive polymeric micelles with core-shell-corona architectures as intracellular anti-cancer drug carriers. *Sci Technol Adv Mater.* 2013;14(4):044402.
- Bellettini IC, Witt MA, Borsali R, Minatti E, Rubira AF, Muniz EC. PS-*b*-PAA nanovesicles coated by modified PEIs bearing hydrophobic and hydrophilic groups. *J Mol Liq.* 2015;210:29-36.
- Burke SE, Eisenberg A. Effect of sodium dodecyl sulfate on the morphology of polystyrene-*b*-poly(acrylic acid) aggregates in dioxane-water mixtures. *Langmuir.* 2001;17(26):8341-7.
- Caon T, Porto LC, Granada A, Tagliari MP, Silva MAS, Simões CMO, et al. Chitosan-decorated polystyrene-*b*-poly(acrylic acid) polymersomes as novel carriers for topical delivery of finasteride. *Eur J Pharm Sci.* 2014;52(1):165-72.
- Choucair A, Lavigneur C, Eisenberg A. Polystyrene-*b*-poly(acrylic acid) vesicle size control using solution properties and hydrophilic block length. *Langmuir.* 2004;20(10):3894-900.
- Discher DE, Eisenberg A. Polymer Vesicles. *Science.* 2002;297(5583):967-73.
- Dong R, Lindau M, Ober CK. Dissociation behavior of weak polyelectrolyte brushes on a planar surface. *Langmuir.* 2009;25(8):4774-9.
- Elgadir MA, Uddin MS, Ferdosh S, Adam A, Chowdhury AJK, Sarker MZI. Impact of chitosan composites and chitosan nanoparticle composites on various drug delivery systems: A review. *J Food Drug Anal.* 2015;23(4):619-29.
- El-Sherbiny IM. Synthesis, characterization and metal uptake capacity of a new carboxymethyl chitosan derivative. *Eur Polym J.* 2009;45(1):199-210.
- Frank LA, Onzi GR, Morawski AS, Pohlmann AR, Guterres SS, Contri RV. Chitosan as a coating material for nanoparticles intended for biomedical applications. *React Funct Polym.* 2020;147.
- Ge HC, Luo DK. Preparation of carboxymethyl chitosan in aqueous solution under microwave irradiation. *Carbohydr Res.* 2005;340(7):1351-6.
- Gong J, Chen M, Zheng Y, Wang S, Wang Y. Polymeric micelles drug delivery system in oncology. *J Controlled Release.* 2012;159(3):312-23.
- Huo M, Zhang Y, Zhou J, Zou A, Yu D, Wu Y, et al. Synthesis and characterization of low-toxic amphiphilic chitosan derivatives and their application as micelle carrier for antitumor drug. *Int J Pharm.* 2010;394(1-2):162-73.
- International Conference on Harmonization. ICH. Q3C (R6) on impurities: guideline for residual solvents. Geneva, Switzerland: ICH; 2019.
- Jung SM, Yoon GH, Lee HC, Jung MH, Yu SI, Min SK, et al. Thermodynamic insights and conceptual design of skin-sensitive chitosan coated ceramide/PLGA nanodrug for regeneration of stratum corneum on atopic dermatitis. *Sci Rep.* 2015;5:1-12.
- Kawashima Y. Nanoparticulate systems for improved drug delivery. *Adv Drug Deliv Rev.* 2001;47(1):1-2.
- Kreuter J. Nanoparticulate systems for brain delivery of drugs. *Adv Drug Deliv Rev.* 2012;64:213-22.
- Liu TY, Chen SY, Lin YL, Liu DM. Synthesis and characterization of amphiphatic carboxymethyl-hexanoyl chitosan hydrogel: Water-retention ability and drug encapsulation. *Langmuir.* 2006;22(23):9740-5.
- Mai Y, Eisenberg A. Self-assembly of block copolymers. *Chem Soc Rev.* 2012;41(18):5969.
- Matos BN, Reis TA, Gratieri T, Gelfuso GM. Chitosan nanoparticles for targeting and sustaining minoxidil sulphate delivery to hair follicles. *Int J Biol Macromol.* 2015;75:225-9.
- Mourya VK, Inamdar NN. Chitosan-modifications and applications: Opportunities galore. *React Funct Polym.* 2008;68(6):1013-51.
- Mura S, Manconi M, Sinico C, Valenti D, Fadda AM. Penetration enhancer-containing vesicles (PEVs) as carriers for cutaneous delivery of minoxidil. *Int J Pharm.* 2009;380(1-2):72-9.
- Ojer P, Iglesias T, Azqueta A, Irache JM, López De Cerain A. Toxicity evaluation of nanocarriers for the oral delivery of macromolecular drugs. *Eur J Pharm Biopharm.* 2015;97(Pt A):206-17.
- Padois K, Cantiéni C, Bertholle V, Bardel C, Pirot F, Falson F. Solid lipid nanoparticles suspension versus commercial solutions for dermal delivery of minoxidil. *Int J Pharm.* 2011;416(1):300-4.
- Qu D, Lin H, Zhang N, Xue J, Zhang C. In vitro evaluation on novel modified chitosan for targeted antitumor drug delivery. *Carbohydr Polym.* 2013;92(1):545-54.
- Sahoo SK, Parveen S, Panda JJ. The present and future of nanotechnology in human health care. *Nanomedicine Nanotechnology, Biol Med.* 2007;3(1):20-31.
- Sica DA. Minoxidil: An underused vasodilator for resistant or severe hypertension. *J Clin Hypertens.* 2004;6(5):283-7.
- Sheng J, Han G, Qin J, Ru G, Li R, Wu L, et al. N-trimethyl chitosan chloride-coated PLGA nanoparticles overcoming

multiple barriers to oral insulin absorption. *ACS Appl Mater Interfaces*. 2015;7(28):15430-41.

Shim J, Kang HS, Park WS, Han SH, Kim J, Chang IS. Transdermal delivery of minoxidil with block copolymer nanoparticles. *J Control Release*. 2004;97(3):477-84.

United States Pharmacopeia. USP. General Chapter <467> Residual Solvents. Rockville, USA: USP; 2007.

Yoon HY, Koo H, Choi KY, Chan Kwon I, Choi K, Park JH, et al. Photo-crosslinked hyaluronic acid nanoparticles with improved stability for *in vivo* tumor-targeted drug delivery. *Biomaterials*. 2013;34(21):5273-80.

Zhang L, Eisenberg A. Multiple morphologies and characteristics of “Crew-Cut” aggregates of polystyrene-*b*-poly(acrylic acid) block copolymers. *Science*. 1995;268(13):1728-31.

Zhang W, Fang S, Liang X. Determination of residual solvents in pharmaceuticals by static headspace gas chromatography using natural deep eutectic solvents as mediums: A partition coefficients study. *Chromatographia*. 2019;82:1523-29.

Zhang X, Ng HLH, Lu A, Lin C, Zhou L, Lin G, et al. Drug delivery system targeting advanced hepatocellular carcinoma: Current and future. *Nanomedicine Nanotechnology, Biol Med*. 2016;12(4):853-69.

Zhang Y, Chan HF, Leong KW. Advanced materials and processing for drug delivery: The past and the future. *Adv Drug Deliv Rev*. 2013;65(1):104-20.

Zhao Y, Brown MB, Jones SA. The effects of particle properties on nanoparticle drug retention and release in dynamic minoxidil foams. *Int J Pharm*. 2010;383(1-2):277-84.

Received for publication on 30th January 2019

Accepted for publication on 23rd April 2020